Electrochemical Pixels: Semi-open electrochemical cells with a vertically stacked design

Marc Clua Estivill, Jhonattan F. Baez [1], Pascal Blondeau, Francisco J. Andrade [*]

Department of Analytical and Organic Chemistry, Universitat Rovira i Virgili, 43007, Tarragona, Spain

ARTICLE INFO

ABSTRACT

A novel electrochemical cell design in a vertically stacked configuration is presented. Through a layered structure using a top macroporous working electrode, a polyelectrolyte, and a bottom metallic conductor a standalone electrochemical cell with an internal reference electrode is built. This sensor allows monitoring an electrochemical property of an external solution with only one electrode in direct contact with the sample. Using paper-based platinum electrode for the porous top electrode and Nafion as polyelectrolyte material, the self-powered detection of hydrogen peroxide is performed. The system can be operated in multiple modes. In a capacitive way, the open circuit potential is measured. Alternatively, in a self-powered current mode, the system emulates a fuel cell. Additionally, a potential-current switched mode is also demonstrated. Because of this unique design and operational features this sensor is considered as an electrochemical pixel. To further demonstrate the advantages of this device, the detection of glucose is performed by building an array of sensors using a single back (reference) electrode and multiple working electrodes. These results lay the groundwork for the development of a new generation of simple and low cost biochemical sensors and electrochemical sensing arrays.

1. Introduction

Detection arrays have become widely popular because of their multiple advantages in terms of enhanced signal to noise ratio, extended detection capabilities and spatial resolution, among many others. For this reason, sensing arrays have been used for decades in spectroscopic devices (Birkinshaw, 1996), and they have been also explored in other areas, such as mass spectrometry (Jungmann and Heeren, 2013). In electrochemical analysis, arrays are also highly attractive when multiple channels of information are required. For example, electrochemical sensing arrays are used in electronic tongues (Cetó et al., 2022) -for food analysis- and in clinical applications, since complex diagnostics require the simultaneous determination of multiple biomarkers. Recently, electrochemical sensing arrays have been proposed for the diagnostic of Alzheimer disease (Song et al., 2020), the detection of hematological tumors (Zhu et al., 2020) and development of point-of-care devices (Gutiérrez-Capitán et al., 2022).

Despite of this significant interest, the evolution of electrochemical sensing arrays has not followed the pace of their spectroscopic counterparts. This is in part due to the strong differences in configuration and operation of their building blocks. In spectroscopic arrays, the minimal independently addressable detection element is often called pixel. Pixels have been miniaturized and designed with a vertically stacked architecture, facilitating the development of densely packed arrays where the top layer contains the sensitive material, and the additional components can be placed underneath. Designing electrochemical arrays with a similar configuration has not been yet possible because of the many unique challenges of (bio)chemical sensors. The need to introduce liquid samples represents a major issue. Also, the fact that virtually all electrochemical sensors require an external reference electrode has been a traditional limitation, even if miniaturization and incorporation of enhanced electronics -such as FET (Sinha and Pal, 2022) or CMOS (Li et al., 2016) technology-has been used. These constrains have favored the widespread adoption of the 2 or 3-electrodes open cell configurations where the sample solution is used also to close the electrical circuit. For this reason, electrochemical arrays have a very vague design that ranges from the simultaneous use of several working electrodes (sharing a common reference electrode) to the use of multiple planar cells (Gao et al., 2016; Timilsina et al., 2021; Wang et al., 2022). As a result, the notion of electrochemical pixel remains elusive. The use of multiple

---

planar electrochemical cells shows a limited sensitive area (out of the total area exposed to the sample) and presents some caveats regarding sample volume and sample introduction. Attempts to solve this issue through miniaturization and simplification of the electrochemical cell have been proposed (Gutiérrez-Capitán et al., 2022), but conventional configurations still show many design and operational limitations.

In this work we present a novel electrochemical cell that emulates the design and operation of a pixel. Quasi solid-state technology in combination with a macroporous working electrode are used to create a semi open electrochemical cell (SOEC) in a vertically stacked configuration. A layered structure made with a bottom electrode, a polyelectrolyte and top macroporous electrode creates a standalone electrochemical cell. It will be shown that one of the most remarkable features of this geometry is that the top electrode can be used to monitor the electrochemical properties of an external solution while using the bottom electrode as internal reference system. This means that only the working electrode is exposed and in direct contact with the sample solution. This reduction of the sensor footprint simplifies the sample introduction and reduces the sample consumption. Furthermore, this SOEC allows the detection of hydrogen peroxide in a fully self-powered approach that can work under different detection schemes: potential, current or switched mode. Last, but not least, it is shown that this novel architecture opens new avenues to build compact electrochemical sensing arrays.

A conceptual diagram of this new device is shown in Fig. 1. First, a metallic conductive material is placed at the bottom, acting as a reference (or counter) electrode. This is the back (or bottom) electrode. Second, a macroporous electrically conductive material is placed at the top, acting as the working electrode. This is the top (or front) electrode. Finally, a polyelectrolyte material (PEM) is used as a separator, creating a third layer in between two electrodes. To be noticed, this PEM also fills the pores of the top electrode. With this configuration, the two electrodes are electrically connected (even in the absence of a sample solution) through the PEM. Because of its porous nature, liquids can be incorporated into the SOEC through the top electrode. Additionally, since these pores are filled with PEM, the outer face of the top electrode is electrically connected with the bottom electrode. This means that when the SOEC is immersed in a solution, the top electrode sits at the interface between the inner cell space and the external solution. Therefore, the electrochemical properties of the outer interface of the top electrode -which can be affected by the solution composition-could be monitored using the bottom electrode as a (pseudo) reference system.

A practical way to create this SOEC is by using Nafion-coated paper-based metal electrodes (Parrilla et al., 2017a). Details on the construction of the cell can be found in the SI. In brief, the top electrode is built by sputtering a thin layer of Pt on one side of a filter paper. The metal-coated cellulose fibers create electrically conductive tracks without occluding the pores of the paper. Then, a solution of a PEM is cast on the metallized side of the paper. For this work, a 5% Nafion solution was used. This solution percolates through the pores and reaches the other side, creating layers of polyelectrolyte on both sides of the paper that are interconnected through the pores. The SOEC is finally assembled by placing the polyelectrolyte-coated metal paper electrode on top of another conductive paper. This creates a layered structure as shown in Fig. 1a. Notably, the metallized side of the top electrode is placed facing outwards. The system is then sealed between two plastic masks, leaving exposed only a 3 mm diameter window. In general, Pt was used for both, top and bottom electrodes. Nevertheless, the bottom electrode can be also made with any other conducting material, such as Ag/AgCl inks, C inks, etc. Once assembled, the SOEC is immersed in a PBS solution. After the hydration of the Nafion, the open circuit potential (OCP) between the front (working) and bottom (reference) electrode assumes a stable value. The OCP of these cells in PBS depends on the material of the back electrode (See Table S1), with the lowest value corresponding to the Pt/Pt SOEC. In all cases, this baseline potential is very stable and show no significant noise or drift.

2. Results and discussions

2.1. Response to peroxide

The SOEC works as standalone electrochemical cell, with an OCP that depends on the difference of electrochemical potential between the top and bottom electrodes. Nevertheless, once immersed in an aqueous solution, this OCP is not just a function of the inner composition of the cell. Since the metallized side of the top electrode is facing outwards, and the PEM-filled pores connect this external side with the inner electrochemical cell, any factor affecting the external electrochemical potential of the top electrode should also affect this internal OCP. In previous works we have shown that a Pt electrode coated with Nafion can be used as a working electrode for the potentiometric sensing of hydrogen peroxide (Parrilla et al., 2017b), a molecule that is the gateway to build a plethora of direct and indirect (labelled) assays. Thus, the SOEC was immersed in a 0.1 M PBS solution and the changes on the OCP upon the addition of increasing concentrations of hydrogen peroxide were monitored (Fig. 2). In all cases, the time traces show a decrease of the OCP with increasing concentrations of peroxide, with a region displaying linear-logarithmic relationship with a sensitivity of 120 mV/decade (Fig. 2D). These results mimic the patterns obtained with conventional electrochemical cells (Cánovas et al., 2017). To further prove this point, a conventional Ag/AgCl reference electrode was placed in the bulk solution and the OCP of the front electrode was simultaneously monitored against the back electrode (internal SOEC OCP) and the external reference electrode (see Fig. S1a). Remarkably,
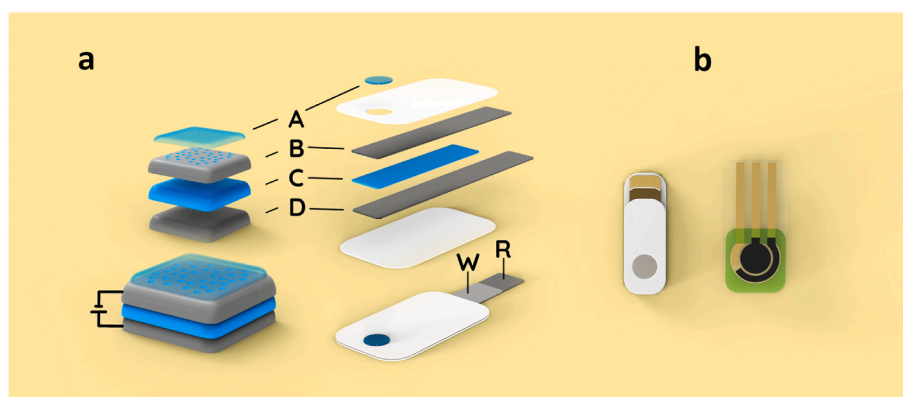
Fig. 1. **a** On the left, schematic representation of the semi-open electrochemical cell (SOEC) with a polyelectrolyte coating (A), a macroporous working electrode (B), a polyelectrolyte material, PEM (C) and a reference (or counter) electrode (D); On the right the typical assembly of the electrodes and the plastic masks with (W) for working and (R) for reference electrode. **b** Assembled SOEC compared to a conventional planar cell. In the SOEC only the working electrode is directly exposed.
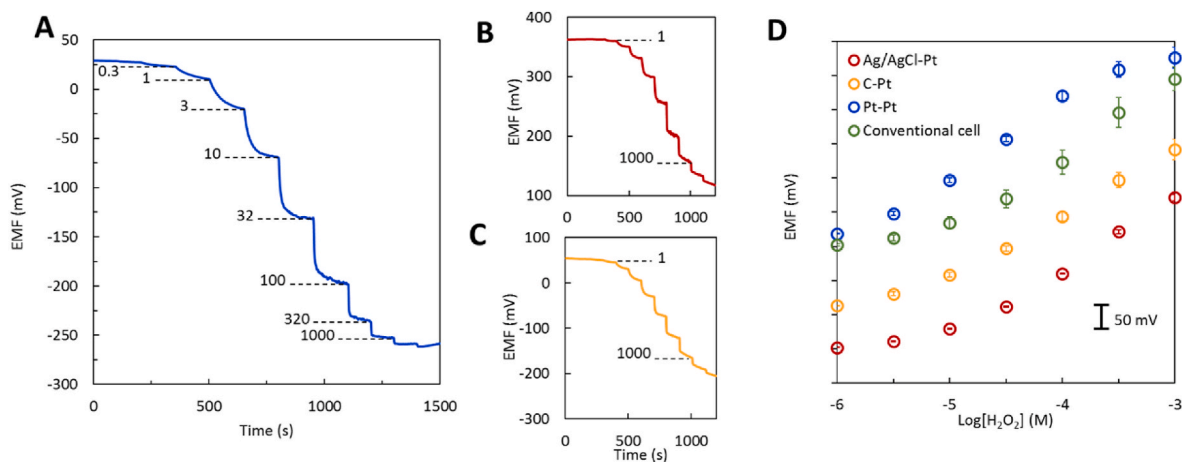
Fig. 2. Time trace of the response to H_2O_2 in PBS 0.1 M pH 7.4 (numbers in the plot indicate the μM concentration of peroxide) of SOECs having a Pt front electrode and back electrodes made of **A)**Pt, **B)** Ag/AgCl **C)** C ink. **D)** Corresponding calibration curves. The response of a conventional electrochemical cell using Nafion-coated platinum paper-based electrode and a 3 M Ag/AgCl/KCl reference electrode. For a better visualization, an offset has been added to the original EMF data. The error bars represent the measurements of 3 sensors (N = 3) and the dashed line represents the linear range.

the results obtained aver similar. The difference in the offset value (Fig. S1b) is due to the different potentials of the reference system. This highlights one of the most unique features of the SOEC, i.e., that the potential of the front electrode can be effectively used monitor a property of an external solution the using the bottom electrode as an internal reference system. This confirms that the porous working electrode and the Nafion bridge can effectively create a functional semi open electrochemical cell for chemical sensing. Using different materials for the bottom electrode creates an offset value of the baseline and may produce a slight shift of the linear ranges but it does not significantly alter the sensitivity (Table S1). Perhaps one of the most surprising results is that even in the Pt/Pt cell the bottom electrode can act as a (pseudo)reference system. In fact, if two separate Pt electrodes are immersed in a PBS solution, the addition of peroxide does not produce any response, as it could be expected (Fig. S2) from any symmetric cell. The asymmetric behavior of the SOEC responds to a combination of factors that involve the relative position of the electrodes and the role of Nafion controlling the transport and the reactivity of peroxide on Pt. it should be also stressed that the system shows good sensor-to-sensor reproducibility, as evidenced by the error bars in Fig. 2D.

2.2. Working principles

In spectroscopic systems the pixel response is the result of a charging photocurrent. By analogy, the SOEC response is also produced by a charging current (but of chemical nature) that is created by the spontaneous reactions of solution components with the metal surface, through a mechanism commonly known as mix potential (Wagner and Traud, 2006), (Hahn et al., 1974). In essence, when a metal contacts a solution that lacks a well-defined redox couple, the gradient of electrochemical potential is balanced by exchanging charges with solution components. Oxidation and reduction reactions create anodic (I_a) and cathodic (I_c) exchange currents -respectively- with a magnitude that depends on the electrode potential. The bottom line is that there is a spontaneous background charge transfer process to and from the solution that shifts the OCP until a steady state is reached (*i.e.*, when both exchange currents reach the same absolute value). Because of the kinetic nature of these redox processes, the electrode potential does not follow a Nernstian dependence, but it is rather described by the Buttler-Volmer formalism. A detailed treatment of this type of systems can be found elsewhere (Park et al., 2013). As an approximation, the Tafel equation can be used to describe the relationship between the electrode potential (*E*) and the exchange current density (*i*) (Shinagawa et al., 2015):

$$E = A\ln(i) + K$$

The parameter K involves a series of system constants (exchange current density, standard potential of the redox reaction, etc.). The value A is known as the Tafel slope ($\frac{RT}{nF}$, where R = universal gas constant, T = absolute temperature, F = Faraday constant) and *n* is the number of electrons involved in the rate limiting step which for a 1 electron process $A = 120$ mV. This equation means that the electrode potential is controlled by chemically mediated charging currents that depend on the reaction mechanisms and the concentration of the species involved. Anything that modifies these currents will force the potential to a new steady state. Mix potential-based chemical sensors using a conventional electrochemical cell have been proposed in the past. Meyerhoff et al. have explored mix potential systems for oxygenated species (Meruva and Meyerhoff, 1995), phosphate (Meruva and Meyerhoff, 1996), etc., while Bard et al. have emphasized the value of this approach and have applied to the detection of metal nanoparticles (Percival and Bard, 2017), with exquisite sensitivity. Our group has shown that a Nafion-coated Pt electrode can be used as a simple and powerful potentiometric sensor for hydrogen peroxide (Baez et al., 2020). In the case of Pt electrodes in aqueous solutions, the oxygen reduction reaction (ORR) is the main factor producing the cathodic exchange current (I_c):

$$O_2 + 4H^+ + 4e^- \rightarrow 2H_2O \qquad \text{(Reaction 1)}$$

The mechanism of this reaction is complex and depends strongly on the reaction conditions. It has been shown that the initial step is the adsorption of O_2 on pristine Pt sites (Markovic, 2002; Si et al., 2014; Zhang and Anderson, 2007)

$$O_2 + 2Pt \leftrightarrow 2Pt(O-O)_{ads} \qquad \text{(Reaction 2)}$$

While there are multiple possible pathways after this initial step, some of which include the generation of hydrogen peroxide as intermediary, the evidence suggests that the transfer of 1 electron to the adsorbed oxygen is the rate-limiting step. The anodic current (I_a) is mostly produced by the water oxidation:

$$H_2O \rightarrow \frac{1}{2}O_2 + 2H^+ + 2e^- \qquad \text{(Reaction 3)}$$

The current created by the ORR removes electrons from the Pt surface, thus forcing the potential to more positive values (Zhou et al., 2012). It is important to stress that Nafion plays a key role enhancing the ORR, which is partially due to the increased local oxygen concentration and reduction of the local pH. (Wang and Lu, 1998), (Parthasarathy

et al., 1992)

Through these reactions is possible to explain the response of the electrode to peroxide (Katsounaros et al., 2012). Mayrhofer et al. have shown that the reaction pathways of peroxide with Pt will depend on the metal surface state, which is dependent on the electrode potential (Katsounaros et al., 2012). From one side, there is a competitive adsorption between O_2 and peroxide for pristine *Pt* sites:

$$H_2O_2 + 2Pt \rightarrow 2Pt(OH) \qquad\qquad \text{(Reaction 4)}$$

Through *Reaction 4* peroxide decomposes on the Pt surface creating adsorbed hydroxylated species. This blocks the first sept of the ORR (*Reaction 2*), thus leading to a decrease on the electrode OCP. When peroxide finds PtO sites it will be oxidized by reducing the metal oxide. This creates an additional anodic process (I_a):

$$H_2O_2 + 2Pt(OH) \rightarrow 2Pt(H_2O) + O_2 \qquad\qquad \text{(Reaction 5)}$$

All these are diffusion-limited reactions. Unfortunately, a rigorous treatment is not possible, since the mechanisms of the reactions of oxygenated species on Pt is a century-old problem that still is being investigated. Michael et al., for example, have recently studied the decomposition of peroxide on Pt (Serra-Maia et al., 2018), and have shown that the particle size and the chemisorbed O_2 has a kinetic effect on the decomposition of peroxide (Serra-Maia et al., 2021). In any case, the oxidation of peroxide can act as an electron-donor process that further contribute to decrease the electrode potential. In summary, peroxide can undergo both, electrochemical and non-electrochemical reactions in Pt surfaces, both of which will have a marked effect on the exchange currents -and therefore the Pt electrode potential-. The actual reaction pathways, *i.e.*, the degree in which Reactions 4 and 5 contribute to the mix potential, will depend on several factors, such as the electrode potential, surface and working conditions, and Pt structure (Fig. 3). Since these are inner core redox reactions, modeling these systems would require an accurate knowledge of the mechanism involved (Percival and Bard, 2017). Furthermore, the role of Nafion -enhancing the reaction kinetics of oxygenated species and modulating the transport of material between top and bottom electrodes-makes the system even more complex. Also, the porous nature of the electrode and the structure of the Pt sputtered on paper add complexity to the system. In any case, these diffusion-limited reactions provide paths for the decomposition of peroxide on the front electrode and can be used to explain why the Pt bottom electrode can act as a reference system. Because of the cell configuration, peroxide should not enter the inner space of the SOEC in a significant degree. Evidently, in the case of the bottom electrode, the potential will depend on the material used. For the
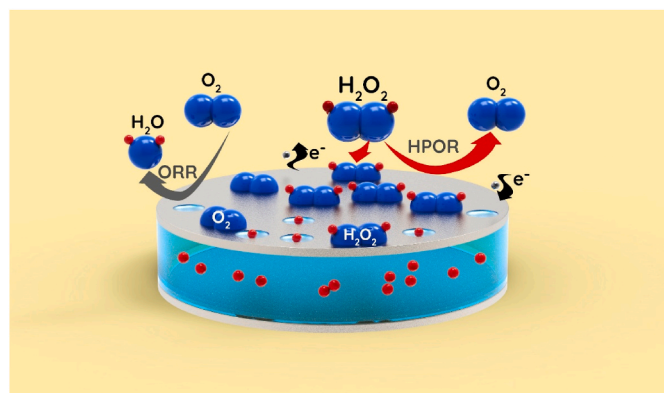
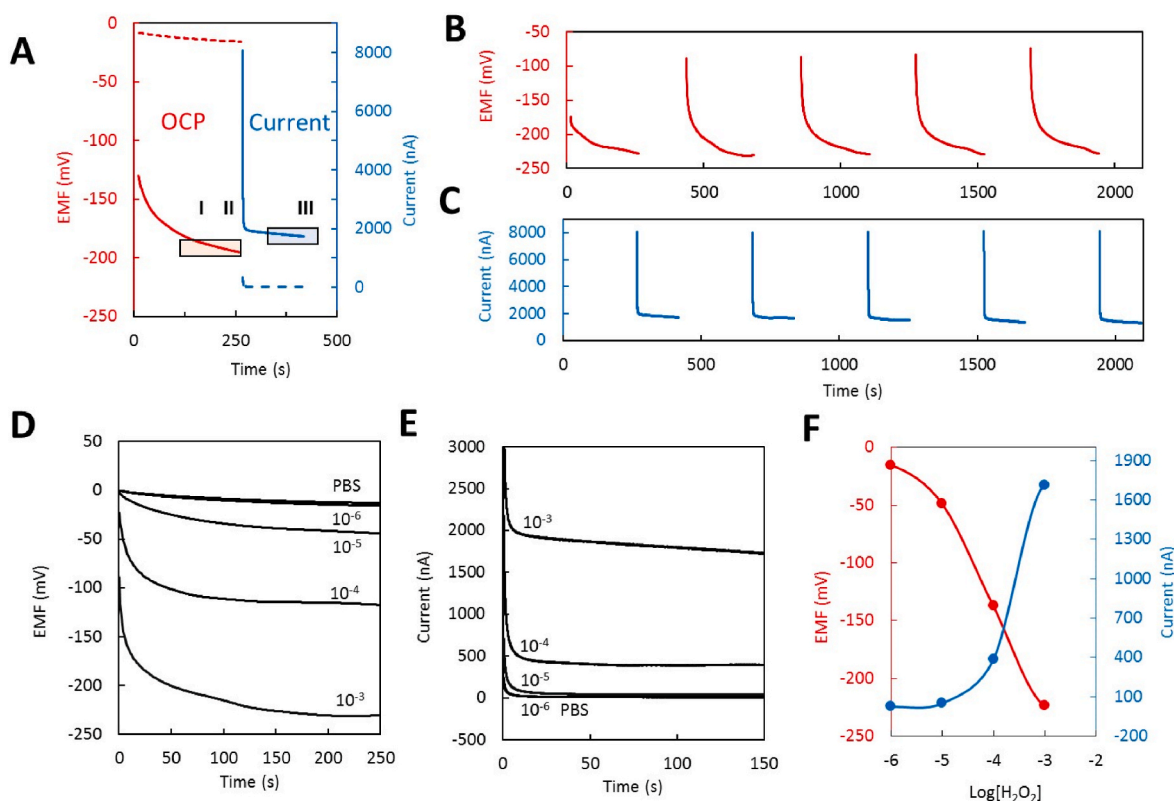rest of the experiments a Pt/Pt system was used.

2.3. Switching operational modes

The Pt/Pt SOEC can be considered -also in analogy with spectroscopic pixels-a (pseudo)capacitively charged device. Initially, both Pt plates (top and bottom electrodes) are subject to similar charging processes produced by a combination of a purely capacitive mechanism -due to the formation of the electric double layer (EDL)- and the Faradaic mix potential reactions described above. These processes lead to a slightly asymmetric pseudocapacitor due to the different local conditions of top and bottom electrodes. The presence of peroxide alters the charging mechanism of the front electrode, which accumulates charges until reaching a new steady state. Therefore, once charged the SOEC can be short circuited, generating a discharge current due to the equilibration of the potential of the two electrodes. If the circuit is re-open, the charging process will start over. This sequence can be repeated several times, producing consecutive charge-discharge cycles as shown in Fig. 4. These time-dependent voltage and current profiles are the result of different interdependent phenomena involving the purely capacitive charging/discharging of the electrode interface together with the potential-dependent redox reactions involved. Both, the OCP that is generated during the charging cycle and the current produced during the discharge cycle show a relationship with the concentration of peroxide. The OCP profile builds up slowly, taking about 250s to reach a steady state (for a 1 mM solution). The current profile, on the other hand, develops much faster and shows two well-defined regions. Immediately after the circuit is closed there is a sharp spike that decays within a few seconds and is followed by a current that stabilizes in a steady state value. These plots show that even for very short times the signal is proportional to the concentration of peroxide. The region where the current assumes a constant value confirms that there is a spontaneous Faradaic process involved. The sign of the current shows that the working electrode is acting as anode, suggesting that this current is due to the oxidation of peroxide (*Reaction 5*). Therefore, the cathodic process in the back electrode is likely due to the ORR (*Reaction 1*), which is largely enhanced due to the presence of Nafion (Parthasarathy et al., 1992). Oxygen is a byproduct of the oxidation of peroxide, and -because of its higher solubility in Nafion-, it could be contributing to the reactions observed. These time profiles are reproducible and can be used to build calibration plots, as shown in Fig. 4. In short, these results show that the SOEC can be operated in a dual mode, alternatively following the potential and the discharge current. Evidently, the charge-based measurements allow for signal integration, thus helping to further enhance the response. Profiles of the total charge (Q) can be seen in Fig. S3.

It's been shown that for the discharge mode the current does not reach the baseline level, but a plateau that depends on the peroxide-concentration. Therefore, experiments were conducted using the SOEC in totally short-circuited mode. In this case the cell behaves like semi-open fuel cell. The addition of peroxide produces stepwise response, with a steady state anodic current increasing with the concentration of peroxide (Fig. 5).

This Faradaic current produced in the short-circuited mode confirms the spontaneous electrochemical decomposition of peroxide, a process in which the Pt structure and its surface state plays a key role. Pt is partially covered by surface oxide layer, with a degree of coverage that depends on the electrode potential. Since peroxide is adsorbed onto pristine Pt sites, but it is oxidized in the PtO sites, the pathways for reactions 1 or 5 will be heavily influenced by the electrode potential. This different reactivity has been the source of many issues in the electrochemical response of Pt to peroxide. Strategies favoring the formation of an oxide layer, such as the application of a positive potential, facilitate the oxidation of peroxide. Nevertheless, the non-spontaneous generation of an oxide layer may lead to the formation of sub-surface oxide layers that lead to irreversible electrode changes. In the SOEC, however, with

Fig. 3. Representation of a cross-section of the SOEC. Region I defines the internal electrochemical cell space, stressing the role of the Nafion bridge and its proton-conducting properties. Region II is the external interface. For visual simplicity, the mix potential reactions have been only represented in the top electrode, but they occur at both platinum surfaces (top and bottom electrodes).

Fig. 4. A) Switched mode: OCP followed by self-powered current measurement of the SOEC. Blank solution (dashed line) and 10^{-3} M [H_2O_2] (solid line), with I: OCP mean value for calibration curve, II: short-circuit to switch to current mode, III: mean value of current for the calibration curve. B) OCP and C) current response for 5 consecutive cycles for a 10^{-3} M [H_2O_2]. D) OCP and E) current response versus time for different concentrations of [H_2O_2] (M). F) Corresponding calibration curves for OCP and current measurements (in the faradaic current region) for the cycle number 2. All measurements have been performed in 0.1 M PBS solution (pH = 7.4).
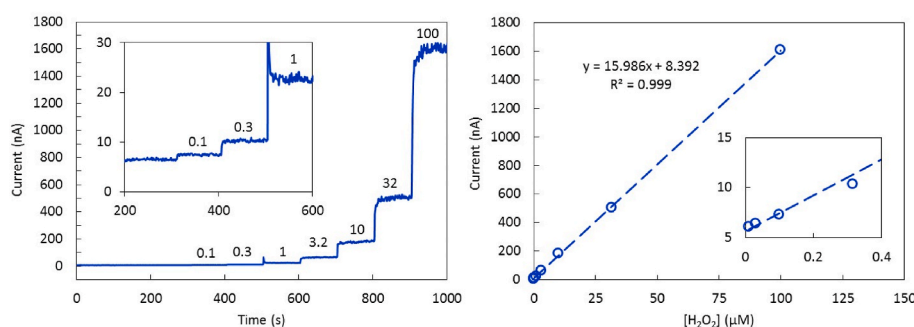
Fig. 5. Time trace of the SOEC upon additions of H_2O_2 in PBS 0.1 M pH 7.4 (left). Numbers in the plot indicate the concentration of peroxide (μM), the inset shows that the response time for a 1 μM addition is approximately 10 s. Right: Corresponding calibration curve of the SOEC (the inset shows the 0–0.5 μM range).

no voltage applied, the surface oxide coverage is enough to show good and reversible response levels (both, potential and current). It is important to mention that the response is highly reversible, i.e., the SOEC can be rinsed and returns to baseline. Thus, any sensor can be reused multiple times obtaining highly reproducible results (Fig. S4). Significant work is still needed to elucidate working mechanisms on this device in which the structure of the sputtered Pt and the use of Nafion have a significant effect.

Optimization of the SOEC performance for both, current and potential mode is currently underway. The results so far show good levels of sensitivity, with linear ranges in the sub-micromolar to hundreds of micromolar of peroxide. Furthermore, in previous works we have shown that the performance of these mix-potential based systems can be tuned by suitable selection of the PEM (Baez et al., 2020). In fact, we have demonstrated the potentiometric detection of glucose in whole,

undiluted blood (among other substances) (Cánovas et al., 2020) using a Nafion-Pt electrode in a conventional cell. One of the most interesting advantages of this device is the compact size of the electrochemical cell, since only one electrode is exposed to the working solution. It is also worth noticing that having the internal reference electrode resting behind the Nafion membrane has two important consequences. First, the reference system is shielded from the matrix. It has been shown that Nafion provides a permselective barriers and minimizes the electrode biofouling. Second, the sample solution is not needed to close the electrical circuit. Once hydrated, the electrode can be removed from the solution and even if the surface is gently dried, the electrical circuit remains closed, and the electrode properties (baseline potential or current) remain unchanged (Fig. S4). All these features should simplify the development of electrochemical tools that must work with untreated samples and require low sample volumes, such as point of care devices.

2.4. From individual pixels to sensing arrays

There is an additional advantage of the SOEC configuration that shows promise in the development of novel sensing platforms. Since the reference electrode is a back plate that lays behind the Nafion coating, several SOEC immersed in the same solution could be sharing the same reference system. In practical terms, this means that the back electrode of each SOEC could be replaced by a single plate that acts as reference system for several sensors. In practical terms, this can be realized by using a large back electrode coated with a layer of Nafion. Over this layer different top (working) electrodes are located (Fig. 6A). In this system the potential of the front electrodes can be individually monitored against a single back plate. To prove this concept, three Pt working electrodes were placed on a single strip of Pt/Nafion paper to create a three-sensor array. First, the calibration of peroxide for the three sensors was performed (Fig. 6B, Figs. S5 and S6). The results obtained for each one of the sensors is similar to that obtained when using the sensors individually. Remarkably, the time traces of Fig. 6B show that the use of a single back plate electrode reduces the sensor-to-sensor variability, which should help in the future to develop more robust calibration approaches. Thereafter, one of the Pt electrodes was functionalized with glucose oxidase (Gox) enzyme. When Glucose is added, only the Gox-functionalized sensor produces a response (Fig. 6C). This means that the peroxide generated by the Gox is not detected by the nearby pixels. This is likely due to the rapid consumption of peroxide on the pixel where is generated, and the dilution effect produced by the solution. This is an important factor when considering pixel cross-talk. Following the addition of glucose, peroxide was added, producing a response in all the three pixels.

These results confirm the feasibility of the SOEC for creating electrochemical dot-matrix arrays using individual top electrodes. The results in Fig. 6 evidence one of the key advantages of these type of systems, which is the simultaneous monitoring of the signal and its baseline level. This should allow, for example, the detection of interferences and the minimization of their effects. Additionally, as it was mentioned above, the simultaneous detection using many functionalized pixels should reduce the need for calibrations and increase the robustness of the determinations. Finally, we are currently developing pixels functionalized with different recognition elements allowing for the simultaneous detection of multiple biomarkers. In this case, an obvious advantage of the SOEC when compared to conventional systems is the significant enhancement of the surface density of sensing units, which leads to a significant decrease of the detection volume. In conventional systems, the cell must accommodate 2 or 3 electrodes, which means that for N target molecules an array must have 2N–3N electrodes in contact with the sample. In the SOEC, only N electrodes are needed. This should

reduce the sample volume and simplify the development of systems that require compact and simple detection, such as wearable and microfluidic devices.

3. Conclusions

This work has introduced a new approach to design an electrochemical cell with a vertically stacked configuration and an internal reference electrode. This has been achieved through the combination of a porous top electrode and polyelectrolyte material. Therefore, unlike conventional sensors where the sample becomes an essential part of the electrochemical cell, this configuration (SOEC) allows the development of a standalone cell with the ability to monitor an external electrochemical property. Because of this unique architecture and operational modes, we have coined this system an electrochemical pixel. The results have shown that this novel design allows may provide several practical advantages, especially in the development of tools for the point of need.

From the design perspective, the use of the macroporous working electrode in combination with a polyelectrolyte material to create the SOEC provides two unique design features. First, the vertically stacked configuration allows the development of compact sensors with only one electrode in direct contact with the sample solution. This geometry should simplify the drop-based and flow-based detection approaches. With only one electrode to contact, the sample volume and the complexity of the sample introduction should be significantly reduced. Second, the use of an internal (pseudo)reference electrode shields the reference system behind a polyelectrolyte membrane, providing ways to enhance the robustness of the sensor. Finally, we have shown that the reduction of the number of electrodes exposed in the surface and the use of a single back plate as a reference electrode facilitates the creation of densely packed electrochemical sensing arrays.

These exceptional design features create unique operational characteristics since the disposition of the electrodes allows the creation of an asymmetric cell behavior. The self-power approach reduces the instrumental complexity (by eliminating external power supplies) and has the potential to enhance the detection (Karyakin et al., 2007). Second, the possibility to operate the system in three modes -potential, current and switched current/potential -increases the versatility of the detection. Last, but not least, the direct detection of peroxide avoids the need of additional enzymes and redox mediators.

The experimental approach employed in this work was meant to provide only a proof of principle of the system. The construction of the working electrode by sputtering metals on paper provides a simple and practical way to create porous electrodes. We are currently exploring the use of nanomaterials -particularly functionalized nano-inks- to improve performance and reduce the amount of material used. Similarly, other
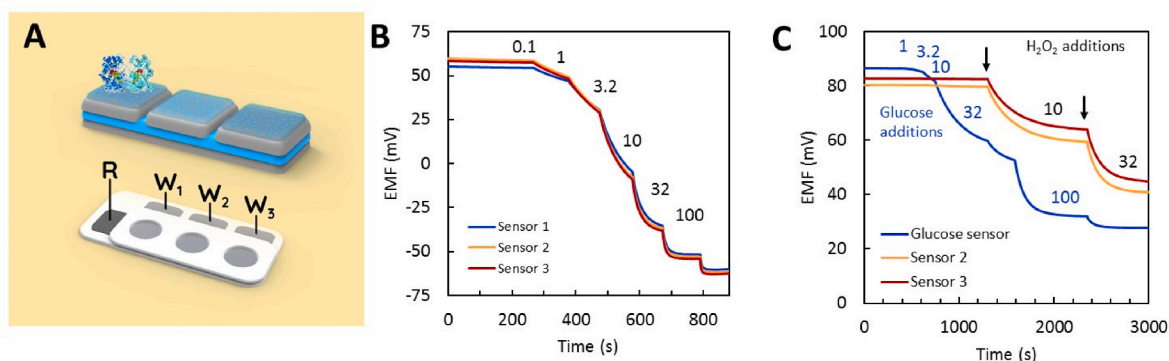
Fig. 6. A) Schematic representation of the SOEC array. Top: diagram of the cells, showing one single back plate and multiple individual top electrodes. Bottom: assembled array, where R is the reference and W_i are the different working electrodes; **B)** Time trace of the SOEC array upon additions of H_2O_2 (numbers in the plot indicate the concentration of peroxide in µM). **C)** Time trace of the SOEC array upon additions of glucose and H_2O_2, i.e. the array consists of a glucose sensor and two peroxide sensors (sensor 2 and 3). First additions of glucose were performed and then hydrogen peroxide was added. All measurements are performed in PBS 0.1 M (pH 7.4).

materials beyond Pt -particularly nanocomposites with controlled reactivity-can help to create electrochemical pixels with different detection capabilities. Methods to control pore geometry and size may further enhance the performance and expand the use of these approach. Regarding the PEM, Nafion is a standard material that shows good performance in solid state electrochemical cells. In previous works we have shown that other materials can be used to modify the performance, and this should be also an area of improvement. Also, the material of the back electrode is another interesting area of research. In all these cases, the work of the sensor in the current and potential mode may require different approaches.

CRediT authorship contribution statement

Marc Clua Estivill: Methodology, Investigation, Writing – review & editing. **Jhonattan F. Baez:** Methodology, Investigation, Writing – review & editing. **Pascal Blondeau:** Methodology, Investigation, Supervision, Writing – review & editing. **Francisco J. Andrade:** Conceptualization, Methodology, Supervision, Resources, Writing – original draft, Writing – review & editing.

Declaration of competing interest

The authors declare the following financial interests/personal relationships which may be considered as potential competing interests:

Francisco J Andrade and Pascal Blondeau report a relationship with EOXSENSE SL, spin-off company of URV that includes: board membership and equity or stocks. Francisco J Andrade and Pascal Blondeau have patent #PCT/EP2021/051075, *PCT/EP2022/072177 and EP23382111.5* pending to URV.

Data availability

Data will be made available on request.

Appendix A. Supplementary data

Supplementary data to this article can be found online at https://doi.org/10.1016/j.bios.2023.115877.

References

Baez, J.F., Compton, M., Chahrati, S., Cánovas, R., Blondeau, P., Andrade, F.J., 2020. Controlling the mixed potential of polyelectrolyte-coated platinum electrodes for the potentiometric detection of hydrogen peroxide. Anal. Chim. Acta 1097, 204–213. https://doi.org/10.1016/j.aca.2019.11.018.

Birkinshaw, K., 1996. Detector arrays in spectroscopy. Int. Rev. Phys. Chem. 15, 13–40. https://doi.org/10.1080/01442359609353172.

Cánovas, R., Blondeau, P., Andrade, F.J., 2020. Modulating the mixed potential for developing biosensors: direct potentiometric determination of glucose in whole, undiluted blood. Biosens. Bioelectron. 163, 112302 https://doi.org/10.1016/j.bios.2020.112302.

Cánovas, R., Parrilla, M., Blondeau, P., Andrade, F.J., 2017. A novel wireless paper-based potentiometric platform for monitoring glucose in blood. Lab Chip 17, 2500–2507. https://doi.org/10.1039/C7LC00339K.

Cetó, X., Pérez, S., Prieto-Simón, B., 2022. Fundamentals and application of voltammetric electronic tongues in quantitative analysis. TrAC Trends Anal. Chem. 157, 116765 https://doi.org/10.1016/j.trac.2022.116765.

Gao, W., Emaminejad, S., Nyein, H.Y.Y., Challa, S., Chen, K., Peck, A., Fahad, H.M., Ota, H., Shiraki, H., Kiriya, D., Lien, D.-H., Brooks, G.A., Davis, R.W., Javey, A., 2016. Fully integrated wearable sensor arrays for multiplexed in situ perspiration analysis. Nature 529, 509–514. https://doi.org/10.1038/nature16521.

Gutiérrez-Capitán, M., Baldi, A., Merlos, Á., Fernández-Sánchez, C., 2022. Array of individually addressable two-electrode electrochemical cells sharing a single counter/reference electrode for multiplexed enzyme activity measurements. Biosens. Bioelectron. 201, 113952 https://doi.org/10.1016/j.bios.2021.113952.

Hahn, P.B., Johnson, D.C., Wechter, M.A., Voigt, A.F., 1974. Mixed-potential mechanism for the potentiometric response of the sodium tungsten bronze electrode to dissolved oxygen and in chelometric titrations. Anal. Chem. 46, 553–558. https://doi.org/10.1021/ac60340a010.

Jungmann, J.H., Heeren, R.M.A., 2013. Detection systems for mass spectrometry imaging: a perspective on novel developments with a focus on active pixel detectors. Rapid Commun. Mass Spectrom. 27, 1–23. https://doi.org/10.1002/rcm.6418.

Karyakin, A.A., Puganova, E.A., Bolshakov, I.A., Karyakina, E.E., 2007. Electrochemical sensor with record performance characteristics. Angew. Chemie Int. Ed. 46, 7678–7680. https://doi.org/10.1002/anie.200700341.

Katsounaros, I., Schneider, W.B., Meier, J.C., Benedikt, U., Biedermann, P.U., Auer, A.A., Mayrhofer, K.J.J., 2012. Hydrogen peroxide electrochemistry on platinum: towards understanding the oxygen reduction reaction mechanism. Phys. Chem. Chem. Phys. 14, 7384. https://doi.org/10.1039/c2cp40616k.

Li, H., Liu, X., Li, L., Mu, X., Genov, R., Mason, A., 2016. CMOS electrochemical instrumentation for biosensor microsystems: a review. Sensors 17, 74. https://doi.org/10.3390/s17010074.

Markovic, N., 2002. Surface science studies of model fuel cell electrocatalysts. Surf. Sci. Rep. 45, 117–229. https://doi.org/10.1016/S0167-5729(01)00022-X.

Meruva, R.K., Meyerhoff, M.E., 1996. Mixed potential response mechanism of cobalt electrodes toward inorganic phosphate. Anal. Chem. 68, 2022–2026. https://doi.org/10.1021/ac951086v.

Meruva, R.K., Meyerhoff, M.E., 1995. Potentiometric oxygen sensing with copper films: response mechanism and analytical implications. Electroanalysis 7, 1020–1026. https://doi.org/10.1002/elan.1140071105.

Park, J.H., Zhou, H., Percival, S.J., Zhang, B., Fan, F.-R.F., Bard, A.J., 2013. Open circuit (mixed) potential changes upon contact between different inert electrodes–size and kinetic effects. Anal. Chem. 85, 964–970. https://doi.org/10.1021/ac3025976.

Parrilla, M., Cánovas, R., Andrade, F.J., 2017a. Paper-based enzymatic electrode with enhanced potentiometric response for monitoring glucose in biological fluids. Biosens. Bioelectron. 90, 110–116. https://doi.org/10.1016/j.bios.2016.11.034.

Parrilla, M., Cánovas, R., Andrade, F.J., 2017b. Enhanced potentiometric detection of hydrogen peroxide using a platinum electrode coated with nafion. Electroanalysis 29, 223–230. https://doi.org/10.1002/elan.201600403.

Parthasarathy, A., Davé, B., Srinivasan, S., Appleby, A.J., Martin, C.R., 1992. The platinum microelectrode/nafion interface: an electrochemical impedance spectroscopic analysis of oxygen reduction kinetics and nafion characteristics. J. Electrochem. Soc. 139, 1634–1641. https://doi.org/10.1149/1.2069469.

Percival, S.J., Bard, A.J., 2017. Ultra-sensitive potentiometric measurements of dilute redox molecule solutions and determination of sensitivity factors at platinum ultramicroelectrodes. Anal. Chem. 89, 9843–9849. https://doi.org/10.1021/acs.analchem.7b01856.

Serra-Maia, R., Bellier, M., Chastka, S., Tranhuu, K., Subowo, A., Rimstidt, J.D., Usov, P. M., Morris, A.J., Michel, F.M., 2018. Mechanism and kinetics of hydrogen peroxide decomposition on platinum nanocatalysts. ACS Appl. Mater. Interfaces 10, 21224–21234. https://doi.org/10.1021/acsami.8b02345.

Serra-Maia, R., Rimstidt, J.D., Michel, F.M., 2021. Kinetic effect of surface chemisorbed oxygen on platinum-catalyzed hydrogen peroxide decomposition. Catal. Lett. 151, 138–146. https://doi.org/10.1007/s10562-020-03280-2.

Shinagawa, T., Garcia-Esparza, A.T., Takanabe, K., 2015. Insight on Tafel slopes from a microkinetic analysis of aqueous electrocatalysis for energy conversion. Sci. Rep. 5, 13801 https://doi.org/10.1038/srep13801.

Si, F., Zhang, Y., Yan, L., Zhu, J., Xiao, M., Liu, C., Xing, W., Zhang, J., 2014. Electrochemical oxygen reduction reaction. In: Xing, W., Yin, G., Zhang, J.B.T.-R.E. M., O,R, E. (Eds.), Rotating Electrode Methods and Oxygen Reduction Electrocatalysts. Elsevier, Amsterdam, pp. 133–170. https://doi.org/10.1016/B978-0-444-63278-4.00004-5.

Sinha, S., Pal, T., 2022. A comprehensive review of FET-based pH sensors: materials, fabrication technologies, and modeling. Electrochem. Sci. Adv. 2, e2100147 https://doi.org/10.1002/elsa.202100147.

Song, Y., Xu, T., Zhu, Q., Zhang, X., 2020. Integrated individually electrochemical array for simultaneously detecting multiple Alzheimer's biomarkers. Biosens. Bioelectron. 162, 112253 https://doi.org/10.1016/j.bios.2020.112253.

Timilsina, S.S., Jolly, P., Durr, N., Yafia, M., Ingber, D.E., 2021. Enabling multiplexed electrochemical detection of biomarkers with high sensitivity in complex biological samples. Acc. Chem. Res. 54, 3529–3539. https://doi.org/10.1021/acs.accounts.1c00382.

Wagner, C., Traud, W., 2006. On the interpretation of corrosion processes through the superposition of electrochemical partial processes and on the potential of mixed electrodes. Corrosion 62, 844–855.

Wang, J., Lu, F., 1998. Oxygen-rich oxidase enzyme electrodes for operation in oxygen-free solutions. J. Am. Chem. Soc. 120, 1048–1050. https://doi.org/10.1021/ja972759p.

Wang, M., Yang, Y., Min, J., Song, Y., Tu, J., Mukasa, D., Ye, C., Xu, C., Heflin, N., McCune, J.S., Hsiai, T.K., Li, Z., Gao, W., 2022. A wearable electrochemical biosensor for the monitoring of metabolites and nutrients. Nat. Biomed. Eng. 6, 1225–1235. https://doi.org/10.1038/s41551-022-00916-z.

Zhang, T., Anderson, A.B., 2007. Oxygen reduction on platinum electrodes in base: theoretical study. Electrochim. Acta 53, 982–989. https://doi.org/10.1016/j.electacta.2007.08.014.

Zhou, H., Park, J.H., Fan, F.-R.F., Bard, A.J., 2012. Observation of single metal nanoparticle collisions by open circuit (mixed) potential changes at an ultramicroelectrode. J. Am. Chem. Soc. 134, 13212–13215. https://doi.org/10.1021/ja305573g.

Zhu, L., Liu, X., Yang, J., He, Y., Li, Y., 2020. Application of multiplex microfluidic electrochemical sensors in monitoring hematological tumor biomarkers. Anal. Chem. 92, 11981–11986. https://doi.org/10.1021/acs.analchem.0c02430.